The kinesin Eg5 drives poleward microtubule flux in *Xenopus laevis* egg extract spindles

David T. Miyamoto,[1] Zachary E. Perlman,[1] Kendra S. Burbank,[1,2] Aaron C. Groen,[1] and Timothy J. Mitchison[1]

[1]Department of Systems Biology, Harvard Medical School, Boston, MA 02115
[2]Department of Physics, Harvard University, Cambridge, MA 02138

Although mitotic and meiotic spindles maintain a steady-state length during metaphase, their antiparallel microtubules slide toward spindle poles at a constant rate. This "poleward flux" of microtubules occurs in many organisms and may provide part of the force for chromosome segregation. We use quantitative image analysis to examine the role of the kinesin Eg5 in poleward flux in metaphase *Xenopus laevis* egg extract spindles. Pharmacological inhibition of Eg5 results in a dose–responsive slowing of flux, and biochemical depletion of Eg5 significantly decreases the flux rate. Our results suggest that ensembles of nonprocessive Eg5 motors drive flux in metaphase *Xenopus* extract spindles.

Introduction

The metaphase spindle is a dynamic structure, balancing continuous antiparallel microtubule sliding, net microtubule polymerization near the midzone, and net depolymerization near the poles (Mitchison, 1989; Sawin and Mitchison, 1991; Brust-Mascher and Scholey, 2002; Maddox et al., 2002). This poleward microtubule flux may provide part of the force for anaphase chromosome movement (Mitchison and Salmon, 1992; Desai et al., 1998; Brust-Mascher and Scholey, 2002; Maddox et al., 2003; Rogers et al., 2004), but its molecular basis is poorly understood. Addition of the nonhydrolyzable ATP analogue AMPPNP stops flux, which could be due to specific inhibition of motors or to a more global perturbation (Sawin and Mitchison, 1991). Recent work has identified a Kin I kinesin as a depolymerization factor involved in flux (Rogers et al., 2004), but it remains unknown whether microtubule depolymerization at the poles drives flux or works in concert with microtubule sliding driven by some other mechanism.

Eg5 is a member of the BimC family of plus end–directed kinesins, which play an important role in the establishment and maintenance of spindle bipolarity (Enos and Morris, 1990; Hagan and Yanagida, 1992; Sawin et al., 1992). Its directionality and gliding rate make Eg5 an attractive candidate for providing the sliding force for flux. Consistent with this hypothesis, Eg5 is a bipolar tetramer in solution and may be capable of sliding apart antiparallel microtubules (Kashina et al., 1996). Specific small molecule inhibitors of Eg5 have been discovered (Mayer et al., 1999; Finer et al., 2001; Hotha et al., 2003) and used to study its role in spindle bipolarity (Kapoor et al., 2000). Preliminary data using a single moderate dose of monastrol did not reveal a role for Eg5 in flux (Kapoor and Mitchison, 2001), but the variability of flux rates in *Xenopus laevis* extract spindles may have hindered the detection of moderate changes in flux rate using standard image analysis techniques. Here, we use a new quantitative analysis technique to enable the rapid, accurate measurement of flux in large numbers of spindles treated with several different Eg5 inhibitors or biochemically depleted of Eg5.

Results and discussion

We used time-lapse fluorescent speckle microscopy (FSM; Waterman-Storer et al., 1998) to visualize the poleward movement of microtubules in metaphase spindles assembled in cell-free *Xenopus* egg extracts (Desai et al., 1999; Video 1, available at http://www.jcb.org/cgi/content/full/jcb.200407126/DC1). We first estimated flux velocities in the presence of Eg5 inhibitors by kymography (Waterman-Storer et al., 1998), in which intensities of speckles along a line in an image are used to generate a distance versus time plot from a time-lapse movie (Fig. 1, A and B). To maintain spindle bipolarity, we relied on the resistance of spindles to collapse in standard coverslip squashes prepared immediately after drug addition (Kapoor and Mitchison, 2001).

Selected kymographs of spindles in the presence of two structurally unrelated inhibitors of Eg5, monastrol (Mayer et al., 1999) or (S)-quinazolinone (Finer et al., 2001; Fig. S1, available at http://www.jcb.org/cgi/content/full/jcb.200407126/DC1), suggested a dose–responsive inhibition of flux (Fig. 1, B, E, and H). However, despite careful control of temperature and

The online version of this article includes supplemental material.

Correspondence to David T. Miyamoto: miyamoto@post.harvard.edu

Abbreviation used in this paper: FSM, fluorescent speckle microscopy.

The Journal of Cell Biology, Vol. 167, No. 5, December 6, 2004 813–818
http://www.jcb.org/cgi/doi/10.1083/jcb.200407126

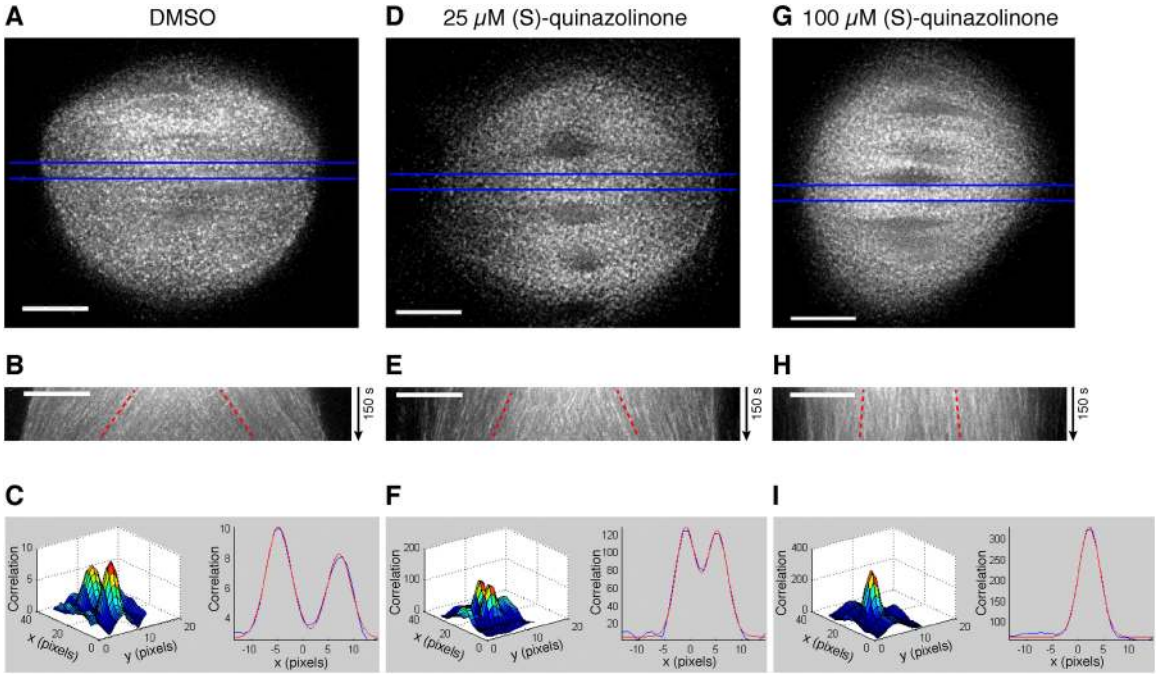

Figure 1. **Pharmacological inhibition of Eg5 decreases the flux rate in a dose–responsive manner.** (A) First frame of a FSM movie showing labeled tubulin in a metaphase spindle in the presence of 1% DMSO (control; see Video 1). Bar, 10 μm. Blue lines outline the region for which kymograph analysis (B) was performed. Red dotted lines are representative traces of speckle streaks, revealing flux. Average flux rate estimated by kymography is 2.21 ± 0.45 μm/min. Bar, 10 μm. (C, left) Average cross-correlation graph for the spindle in A for intervals of 25 s between frame pairs. The two peaks reflect two speckle populations that moved apart due to poleward flux. (right) Blue line is the correlation value along the plane bisecting the two maxima of the cross-correlation graph. Red line is the best fit curve using a two-Gaussian distribution. The distance between the centers of the two peaks reports on the flux rate. Average flux rate measured by cross-correlation is 1.97 ± 0.16 μm/min. (D–F) Same as A–C, in the presence of 25 μM (S)-quinazolinone (see Video 2). Flux rate is slowed (1.32 ± 0.37 μm/min by kymography, 1.02 ± 0.01 μm/min by cross-correlation). (G–I) Same as A–C, in the presence of 100 μM (S)-quinazolinone (see Video 3). Flux rate is almost completely inhibited (0.32 ± 0.33 μm/min by kymography, <0.2 μm/min by cross-correlation). Videos are available at http://www.jcb.org/cgi/content/full/jcb.200407126/DC1.

other external variables, we observed considerable variation in flux rates. We also noted that manual analysis of velocities from kymographs sampled a small subset of speckles in the spindle and introduced a measurement bias toward tracking bright and long-lived speckles, making it difficult to objectively assess the effect of Eg5 inhibitors on flux.

We developed an automated method based on cross-correlation (Westerweel, 1997) to enable the rapid measurement of average whole spindle flux rates in large numbers of spindles. In brief, if a group of speckles in a spindle move poleward at similar velocities, their positions relative to each other will not vary over short times. The cross-correlation algorithm uses this persistent pattern to find the change in position of a group of speckles over some time interval. In a bipolar spindle with antiparallel microtubules sliding poleward, two populations of speckles move away from each other. This results in two cross-correlation maxima, and the distance between these reports on the average flux rate (Fig. 2 A and see Materials and methods). The average flux rates measured by cross-correlation and estimated from kymography were similar in a wide range of control and Eg5-inhibited spindles (Fig. 1, B and C, E and F, and H and I; and Fig. 2, B and C). This fast ensemble-based method samples a larger data set from each spindle than manual kymography and can analyze short movies to calculate speckle velocities (20 s for control spindles and 90 s for slowed spindles), whereas visual kymograph analysis generally requires significantly longer movies. Thus, we were able to considerably increase the number of spindles and perturbation conditions we could sample and accurately measure in each experiment.

We used cross-correlation to measure average flux rates in short time-lapse movies of Eg5 inhibitor-treated spindles. We performed multiple dose–response series and measured multiple spindles at each dose to account for the considerable variation in flux rates within samples (Fig. 2 D). Flux rates decreased with increasing doses of both monastrol and (S)-quinazolinone (Fig. 3 A and Fig. S2 A, available at http://www.jcb.org/cgi/content/full/jcb.200407126/DC1). A simple hyperbolic curve reflecting noncooperative drug binding closely fit the dose–response relationship we observed.

To control for the possibility that coverslip-mediated rescue of collapse itself slowed flux in the presence of Eg5 inhibitors, we sought an alternative method for preventing spindle collapse. We recently discovered that spindles treated with the dynein-dynactin inhibitor p50/dynamitin (Wittmann and Hyman, 1999; "p50 spindles") remain bipolar in solution after inhibition of Eg5 (unpublished data). Because p50 spindles exhibit normal flux in the absence of other perturbations (Shirasu-Hiza et al., 2004; Fig. 3 B), we measured the effects of Eg5 inhibitors on flux in p50 spindles. p50 spindles were incubated with inhibitor in solution for at least 30 min to ensure that the rates measured were not the result of slowed collapse. Flux in trapped and p50 spindles responded similarly to Eg5 inhibition (Fig. 3 and

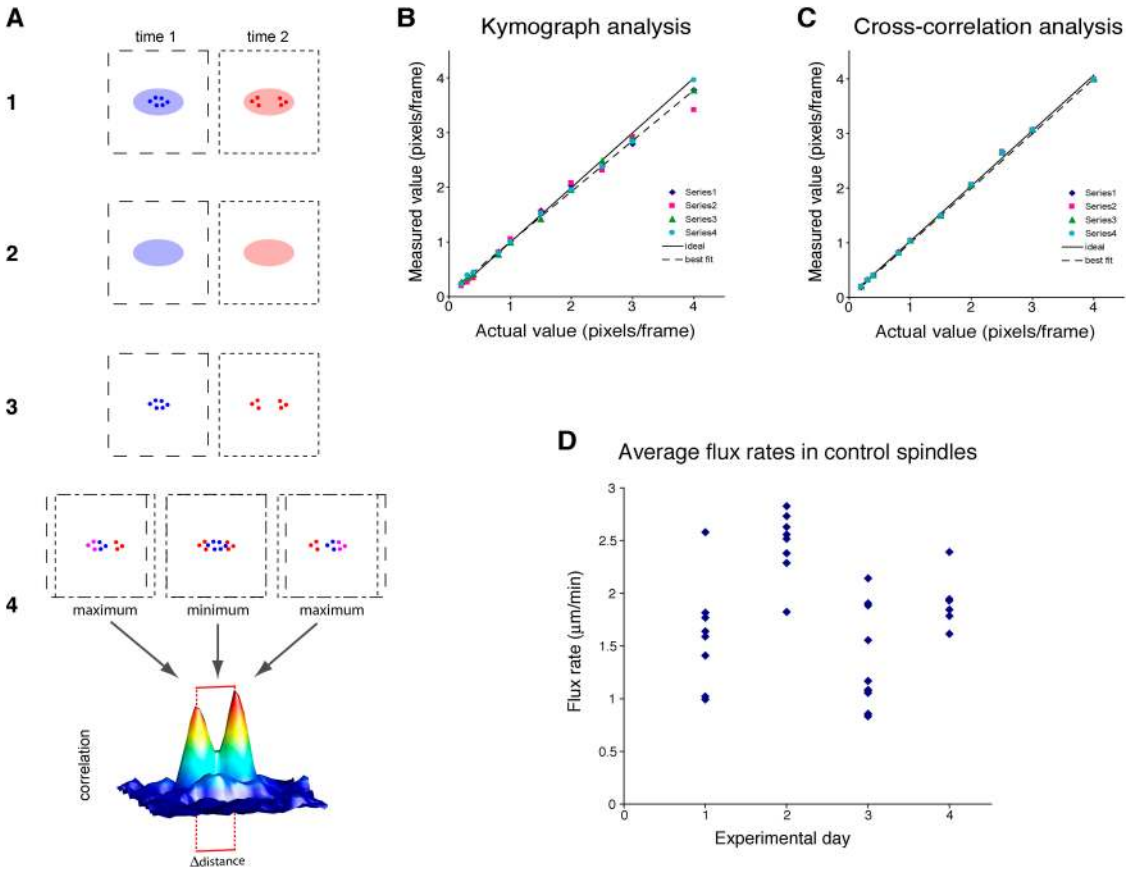

Figure 2. **Rapid automated measurements reveal the high variability of average flux rates in *Xenopus* extract spindles.** (A) Schematic of cross-correlation algorithm (see Materials and methods). In brief, images (1) are filtered and background images (2) are subtracted to emphasize speckles (3), and the cross-correlation (4) is computed. The two peaks surrounding the cross-correlation maxima are fit to the sum of two Gaussians, allowing a subpixel resolution determination of the average rate of movement of speckle ensembles. (B and C) Validation of cross-correlation using simulated speckle data (see Materials and methods). See Video 4 for a sample movie. (B) Results of kymograph analysis of four sets of data simulated for a series of velocities. The linear least squares fit is described by $y = 0.930x + 0.0705$, $R^2 = 0.995$. (C) Results of cross-correlation analysis of the same four sets of data. The linear least squares fit is described by $y = 1.01x + .0122$, $R^2 = 0.999$. (D) Average flux rates in control spindles from four different extract days, measured using cross-correlation analysis. Each point represents a separate spindle.

Fig. S2). The IC_{50} for inhibition of flux by monastrol and (S)-quinazolinone were similar in both trapped and p50 spindles and matched the IC_{50} for inhibition of spindle bipolarity, suggesting that the same activity is being inhibited in all cases (Table I). We note these IC_{50} values are higher than those reported in pure protein assays (IC_{50} for in vitro Eg5 activity: ~14 μM for monastrol and <100 nM for (S)-quinazolinone; Mayer et al., 1999; Finer et al., 2001), an effect we attribute to compound sequestration by membranes, which are abundant in extracts. Consistent with this finding, the degree of difference is mirrored in the calculated n-octanol/water partition coefficients (cLogP = 2 for monastrol; cLogP = 6 for quinazolinone). The (R)-enantiomer of the quinazolinone, which has a negligible effect on Eg5 ATPase activity in vitro (Maliga, Z., personal communication), had no effect on flux or spindle bipolarity (Table I). A potent derivative of another structurally unrelated Eg5 inhibitor, HR22C16 (Hotha et al., 2003), also slowed flux in a dose–responsive manner (unpublished data). These pharmacological data strongly suggest that specific inhibition of Eg5 slows flux.

These results suggest that Eg5 drives flux, but could also be explained if pharmacological inhibition of Eg5 induces a braking effect on microtubule sliding. We consider such an effect unlikely because monastrol-inhibited Eg5 does not dramatically slow microtubule gliding driven in vitro by conventional kinesin (Crevel et al., 2004). To directly address the possibility of braking and to further test specificity, we measured the effects on flux of Eg5 immunodepletion in p50 spindles (Fig. 4). Three sequential rounds of depletions were required to remove >99% of Eg5 from extracts. As expected, cycled spindle assembly in Eg5-depleted extract primarily gave monoasters, whereas mock depletion gave mostly bipolar spindles (Fig. 4 B). Addition of p50/dynamitin to Eg5-depleted extracts rescued bipolarity (Fig. S3 C, available at http://www.jcb.org/cgi/content/full/jcb.200407126/DC1; unpublished data). Measurement by kymography and cross-correlation showed that mock-depleted spindles fluxed at a normal rate (not depicted), as did mock-depleted spindles treated with p50/dynamitin (Fig. 4 C; and Fig. S3, A and B). However, p50 spindles assembled in Eg5-depleted extract showed a significantly slowed flux rate despite the rescue of spindle bipolarity (Fig. 4 C; and Fig. S3, C and D). Purified recombinant full-length Eg5, which restored spindle bipolarity in Eg5-depleted extract (Fig. 4,

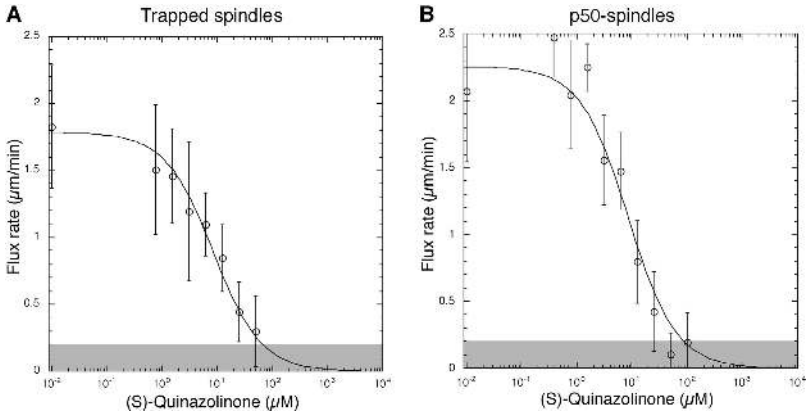

Figure 3. **Flux rates show similar dose–response to inhibition of Eg5 when spindle collapse is suppressed by either mechanical or biochemical means.** (A) Dose–response of flux to (S)-quinazolinone in physically trapped spindles (n = 189 spindles from three dosage series done on three different days; each point represents the average flux rate from >20 spindles). (B) Dose–response of flux to (S)-quinazolinone when spindle collapse is prevented in solution by addition of p50/dynamitin (n = 114 spindles from two dosage series done on two different days; each point represents the average flux rate from >10 spindles). Error bars show SD. The gray area indicates the lower bound of velocity resolvable by the cross-correlation method (see Materials and methods). The line is a best-fit hyperbolic inhibition curve, $R^2 = 0.98$ for A and $R^2 = 0.94$ for B.

A and B), partially rescued flux in Eg5-depleted p50 spindles (Fig. 4 C; and Fig. S3, E and F).

In sum, three structurally unrelated inhibitors of Eg5 slowed flux in a dose–responsive manner under two different methods of maintaining bipolarity, and immunodepletion of Eg5 caused a significant slowing of flux in p50 spindles that can be partially rescued by addition of recombinant protein. Eg5 activity is thus required for normal flux and might directly drive microtubule sliding. This finding may appear to contradict a previous study in which some bipolar spindles that formed in Eg5-depleted extract fluxed normally (Sawin and Mitchison, 1994). We believe that Eg5 was not efficiently depleted in that study, which used only a single round of immunodepletion. We speculate that the remaining Eg5 assembled cooperatively onto spindles that achieved bipolarity, allowing normal flux. Even in the current work, near complete Eg5 depletion did not completely block flux, although very high doses of Eg5 inhibitor completely halt sliding (unpublished data). However, it remains possible that other plus end–directed motors or regulators of microtubule dynamics contribute to flux.

The simple hyperbolic dose–response curve we observed suggests that the speed of microtubule sliding is proportional to the concentration of active motor. If the flux rate is limited not by load but rather by the maximal velocity of Eg5 motors, as suggested by the similarity of flux rates and in vitro gliding rates (Sawin et al., 1992; Kapoor and Mitchison, 2001), then such a proportional relationship may suggest that Eg5 in the spindle behaves as a nonprocessive motor, because processivity would yield a nonlinear relationship between motor density and gliding velocity (Howard, 2001). Consistent with this hypothesis, Eg5 appears to be nonprocessive in vitro (Crevel et al., 1997). Flux in extract spindles may thus be driven by ensembles of Eg5 acting nonprocessively, and the variability of flux rates between extract spindles might reflect differing amounts of Eg5.

Eg5 is likely to act on antiparallel microtubules, and therefore on overlapping interpolar microtubules. Flux rates vary among different animal cells, possibly reflecting differing ratios of interpolar microtubules to kinetochore fibers. Most of the microtubules in *Xenopus* extract spindles appear to be of the overlap class, and these spindles may therefore be dominated by Eg5-driven flux. Consistent with an essential role for antiparallel overlap in this system, we have recently used FSM to show that monopolar CSF extract spindles do not flux and that the onset of flux correlates with the onset of bipolar organization (Mitchison et al., 2004). In contrast, kinetochore fibers, which have uniform microtubule polarity, may flux by different mechanisms. For example, detached and isolated kinetochore fibers in grasshopper spermatocyte spindles flux in the apparent absence of antiparallel neighbors (Chen and Zhang, 2004). The mechanistic differences between parallel and antiparallel microtubules are highlighted by measurements indicating that kinetochore fibers flux slower than overlap microtubules (Waterman-Storer et al., 1998; Maddox et al., 2003). A better understanding of the behaviors of microtubule subpopulations in spindles will require extensive comparative FSM studies using nonaveraging measurement techniques (Vallotton et al., 2003). The techniques we introduce in this paper may be useful for addressing the role of Eg5 in flux in other organisms as well as in anaphase in *Xenopus* extract spindles.

Early models suggested that poleward microtubule flux occurs by a treadmilling mechanism in which sliding is driven by differences in tubulin subunit affinity at opposite ends of the microtubule (Margolis et al., 1978). Our data demonstrate that Eg5 activity is required for flux in *Xenopus* extract spindles and suggests a model in which ensembles of Eg5 drive sliding by exerting force between antiparallel microtubules. This sliding may be coupled to plus end dynamic instability and depolymerization at poles by the action of Kin I kinesins (Rogers et al., 2004), accounting for poleward microtubule flux. The role of flux in chromosome movement and spindle assembly are open questions that can be addressed now that the sliding motor has been identified.

Table I. **Eg5 inhibitors exhibit similar IC_{50} values for flux and spindle bipolarity**

Compound	IC_{50} for flux in trapped spindles	IC_{50} for flux in p50 spindles	IC_{50} for spindle bipolarity
	μM	μM	μM
(S)-quinazolinone	8.5 ± 0.5	8.6 ± 0.8	12 ± 4.8
(R)-quinazolinone	>200	ND	>200
Monastrol	28 ± 2.5	30 ± 4.2	31 ± 11

IC_{50} values (±SEM) for inhibition of flux and for inhibition of spindle bipolarity by Eg5 inhibitors were calculated by fitting a simple hyperbolic inhibition curve to dose–response data using nonlinear regression.

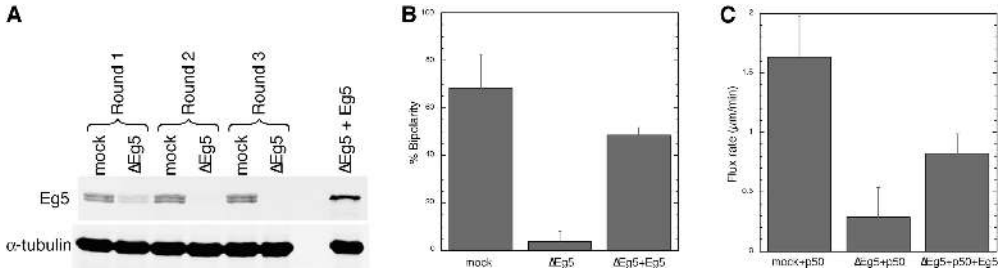

Figure 4. **Immunodepletion of Eg5 significantly decreases the flux rate.** (A) Western blot for Eg5 in *Xenopus* extracts over three sequential rounds of immunodepletion using either anti-Eg5 antibody or nonimmune IgG. Right-most lane shows extract triple-depleted of Eg5 and supplemented with full-length, recombinant Eg5 (twice the endogenous concentration). α-Tubulin Western blot is a loading control. (B) Percentage of spindles that are bipolar when assembled in mock-depleted extract, Eg5-depleted extract, and Eg5-depleted extract supplemented with recombinant full-length Eg5. Values are the averages from three independent experiments, with >100 spindles per condition counted for each experiment. Error bars show SD. (C) Flux rates measured by cross-correlation for p50 spindles assembled in mock-depleted extract, Eg5-depleted extract, and Eg5-depleted extract supplemented with recombinant full-length Eg5 (n = 29 spindles for mock+p50, n = 35 spindles for ΔEg5+p50, and n = 26 spindles for ΔEg5+p50+Eg5, from three independent experiments). Error bars show SD.

Materials and methods

Spindle assembly and FSM

We prepared *Xenopus* egg extracts as described and spindles were assembled after one cycle of DNA replication (Desai et al., 1999). We performed FSM as described using X-rhodamine–labeled tubulin (Waterman-Storer et al., 1998). Images were acquired at 20°C on a microscope (model E800; Nikon) with 60× or 100× objective (1.4 NA Plan Apo DIC; Nikon), immersion oil (Deltavision), and cooled CCD camera (MicroMax; Princeton Instruments) using Metamorph Imaging software (Universal Imaging Corp.). 4 μl of spindle reactions were squashed under 18 × 18-mm coverslips and imaged by wide field microscopy with the focal plane in the middle of each spindle. We typically acquired movies of 4–6 spindles per coverslip, 18 frames each, 5-s intervals, and 400 ms exposure. In some cases, 2–3 movies of 25 to 40 frames at 5-s intervals were acquired. We saw no correlation between flux rate and extract age or time spent under glass.

Inhibitor studies

Monastrol (Mayer et al., 1999) and (S)- and (R)-quinazolinone (Fig. S1; Finer et al., 2001) were prepared as described previously (gift from Z. Maliga, Harvard Medical School, Boston, MA). HR22C16-A2 was a gift from T. Kapoor (Rockefeller University, New York, NY). We prepared 100× DMSO stocks of each dilution for each compound. For trapped spindle studies, we added 0.5 μl of compound stock to 50 μl of preassembled spindles before rapid squash preparation. For p50 spindles, we added 0.7–1 mg/ml p50/dynamitin (Wittmann and Hyman, 1999) at the time of CSF addback (Desai et al., 1999) or after spindle assembly. Compounds were added to p50 spindle reactions and incubated at least 30 min before squash preparation. Untreated controls were prepared periodically to detect any gross variation in flux rate over time. For spindle collapse studies, we added compounds to preassembled spindles and incubated for 30 min before taking fixed squashes. We counted >100 spindles per treatment and calculated percent bipolarity.

Immunodepletion studies

Rabbit polyclonal antibodies were affinity purified against Eg5 tail construct GT-Eg5T (Sawin et al., 1992) after depletion of anti-GST antibody. Immunodepletions were done with Dynabeads (Dynal) as described previously (Desai et al., 1999), with three successive rounds needed to render Eg5 undetectable. p50/dynamitin (Wittmann and Hyman, 1999) was added at the time of CSF addback. Full-length recombinant 6-His–tagged *Xenopus* Eg5 was purified from SF9 cells as described previously, confirmed functional in gliding assays (Kapoor and Mitchison, 2001), and flash-frozen. Freeze-thawed Eg5 appeared partially aggregated by analytical gel filtration, but rescued spindle bipolarity in Eg5-depleted extracts. Recombinant Eg5 was added to Eg5-depleted extracts on ice before spindle assembly after clarifying for 15 min at 20,800 *g* at 4°C. Eg5 concentrations were measured in depleted extracts by quantitative Western blots using an Odyssey Infrared Imaging System (LI-COR Biosciences).

Kymograph and cross-correlation analysis

For kymographs, movies were often aligned using a cross-correlation–based image registration algorithm (Mitchison et al., 2004), but in all cases rotated by cubic interpolation to the horizontal axis to avoid dilation of pixels in the resultant kymograph (Metamorph Imaging software; Universal Imaging Corp.). Kymographs were prepared after applying an unsharp mask filter as described previously (Waterman-Storer et al., 1998). Flux rates were calculated from slopes of speckle trajectories.

Cross-correlation measurement of average speckle velocity with sub-pixel precision used a strategy similar to particle image velocimetry techniques (Westerweel, 1997). We wrote analysis software in Matlab (Mathworks); code and documentation is available at http://mitchison.med.harvard.edu. Each movie was cropped to the edges of the spindle and bandpass filtered to remove shot noise and large overall variations in image intensity. We manually determined a relevant time interval i and computed the cross-correlation for all possible (t, $t + i$) pairs by conjugate multiplication in the Fourier domain. We generally saw two peaks, reflecting speckle movement toward opposite poles. For control spindles, we used intervals of three, four, and five frames (15, 20, and 25 s). For spindles with slower flux rates, we used intervals up to 17 frames (85 s) to maintain separation of cross-correlation peaks. For each interval, all frame-pair cross-correlations were averaged. We found the line of highest integrated value using a Radon transform and fit the resulting profile as a sum of two Gaussians. The distance between centers of the Gaussians reflects the difference in displacement of the two speckle ensembles. Dividing by the time interval yields twice the flux rate. Rates were checked for consistency across the three to five best pair intervals.

Flux rates calculated by cross-correlation were consistent with average flux rates obtained by manual kymograph analysis (Figs. 1 and 2). The analysis was further validated using simulated data. Random distributions of "fluorophores" were individually moved at each step in a time series according to velocities drawn from a normal distribution, and simulated images were generated for each time by convolving the fluorophore distribution with a point-spread function. See Video 4 (available at http://www.jcb.org/cgi/content/jcb.200407126/DC1) for a sample simulated movie. Analysis of these simulations suggests that cross-correlation can resolve velocities with a lower bound of 0.2 μm/min, assuming a microtubule turnover rate of 60–90 s. For dose–response analysis, a flux rate of zero was assigned to all spindles for which rates were not resolvable.

Online supplemental material

Chemical structures of Eg5 inhibitors, flux dose–response data for monastrol, and kymographs from Eg5 depletion-addback experiments are provided. Three movies corresponding to Fig. 1 and one movie showing a sample simulated speckle time-lapse sequence are also included. Online supplemental material is available at http://www.jcb.org/cgi/content/jcb.200407126/DC1.

We thank E.D. Salmon, T. Kapoor, and the Marine Biological Laboratory Cell Division Group for inspiring this project and useful discussions. We thank T. Kapoor for HR22C16-A2 and GT-Eg5T DNA construct, C. Walczak for helpful discussions on antibody production, and Z. Maliga for Eg5 inhibitors.

We thank W. Brieher, G. Charras, R. Ward, M. Shirasu-Hiza, A. Vrabioiu, and Z. Maliga for critical reading of the manuscript.

This work was supported by grants from the National Institutes of Health to T.J. Mitchison. D.T. Miyamoto and Z.E. Perlman are Howard Hughes Medical Institute Predoctoral Fellows, and A.C. Groen is a National Science Foundation Predoctoral Fellow.

Submitted: 19 July 2004
Accepted: 29 September 2004

References

Brust-Mascher, I., and J.M. Scholey. 2002. Microtubule flux and sliding in mitotic spindles of *Drosophila* embryos. *Mol. Biol. Cell.* 13:3967–3975.

Chen, W., and D. Zhang. 2004. Kinetochore fibre dynamics outside the context of the spindle during anaphase. *Nat. Cell Biol.* 6:227–231.

Crevel, I.M., A. Lockhart, and R.A. Cross. 1997. Kinetic evidence for low chemical processivity in ncd and Eg5. *J. Mol. Biol.* 273:160–170.

Crevel, I.M., M.C. Alonso, and R.A. Cross. 2004. Monastrol stabilises an attached low-friction mode of Eg5. *Curr. Biol.* 14:R411–R412.

Desai, A., P.S. Maddox, T.J. Mitchison, and E.D. Salmon. 1998. Anaphase A chromosome movement and poleward spindle microtubule flux occur at similar rates in *Xenopus* extract spindles. *J. Cell Biol.* 141:703–713.

Desai, A., A. Murray, T.J. Mitchison, and C.E. Walczak. 1999. The use of *Xenopus* egg extracts to study mitotic spindle assembly and function in vitro. *Methods Cell Biol.* 61:385–412.

Enos, A.P., and N.R. Morris. 1990. Mutation of a gene that encodes a kinesin-like protein blocks nuclear division in *A. nidulans*. *Cell.* 60:1019–1027.

Finer, J.T., G. Bergnes, B. Feng, W.W. Smith, and J.C. Chabala. 2001. Methods and compositions using quinazolinones. *In* World Intellectual Property Organization. Vol. WO 01/30768 A. http://www.wipo.int/pct/en/ (accessed July 19, 2004.

Hagan, I., and M. Yanagida. 1992. Kinesin-related cut7 protein associates with mitotic and meiotic spindles in fission yeast. *Nature.* 356:74–76.

Hotha, S., J.C. Yarrow, J.G. Yang, S. Garrett, K.V. Renduchintala, T.U. Mayer, and T.M. Kapoor. 2003. HR22C16: a potent small-molecule probe for the dynamics of cell division. *Angew. Chem. Int. Ed. Engl.* 42:2379–2382.

Howard, J. 2001. Speeds of motors. *In* Mechanics of Motor Proteins and the Cytoskeleton. Sinauer Associates, Inc., Sunderland, MA. 213–227.

Kapoor, T.M., and T.J. Mitchison. 2001. Eg5 is static in bipolar spindles relative to tubulin: evidence for a static spindle matrix. *J. Cell Biol.* 154: 1125–1133.

Kapoor, T.M., T.U. Mayer, M.L. Coughlin, and T.J. Mitchison. 2000. Probing spindle assembly mechanisms with monastrol, a small molecule inhibitor of the mitotic kinesin, Eg5. *J. Cell Biol.* 150:975–988.

Kashina, A.S., R.J. Baskin, D.G. Cole, K.P. Wedaman, W.M. Saxton, and J.M. Scholey. 1996. A bipolar kinesin. *Nature.* 379:270–272.

Maddox, P., A. Desai, K. Oegema, T.J. Mitchison, and E.D. Salmon. 2002. Poleward microtubule flux is a major component of spindle dynamics and anaphase a in mitotic *Drosophila* embryos. *Curr. Biol.* 12:1670–1674.

Maddox, P., A. Straight, P. Coughlin, T.J. Mitchison, and E.D. Salmon. 2003. Direct observation of microtubule dynamics at kinetochores in *Xenopus* extract spindles: implications for spindle mechanics. *J. Cell Biol.* 162: 377–382.

Margolis, R.L., L. Wilson, and B.I. Keifer. 1978. Mitotic mechanism based on intrinsic microtubule behaviour. *Nature.* 272:450–452.

Mayer, T.U., T.M. Kapoor, S.J. Haggarty, R.W. King, S.L. Schreiber, and T.J. Mitchison. 1999. Small molecule inhibitor of mitotic spindle bipolarity identified in a phenotype-based screen. *Science.* 286:971–974.

Mitchison, T.J. 1989. Polewards microtubule flux in the mitotic spindle: evidence from photoactivation of fluorescence. *J. Cell Biol.* 109:637–652.

Mitchison, T.J., and E.D. Salmon. 1992. Poleward kinetochore fiber movement occurs during both metaphase and anaphase-A in newt lung cell mitosis. *J. Cell Biol.* 119:569–582.

Mitchison, T.J., P. Maddox, A. Groen, L. Cameron, Z. Perlman, R. Ohi, A. Desai, E.D. Salmon, and T.M. Kapoor. 2004. Bipolarization and poleward flux correlate during *Xenopus* extract spindle assembly. *Mol. Biol. Cell.* doi:10.1091/mbc.E04-05-0440.

Rogers, G.C., S.L. Rogers, T.A. Schwimmer, S.C. Ems-McClung, C.E. Walczak, R.D. Vale, J.M. Scholey, and D.J. Sharp. 2004. Two mitotic kinesins cooperate to drive sister chromatid separation during anaphase. *Nature.* 427:364–370.

Sawin, K.E., and T.J. Mitchison. 1991. Poleward microtubule flux mitotic spindles assembled in vitro. *J. Cell Biol.* 112:941–954.

Sawin, K.E., and T.J. Mitchison. 1994. Microtubule flux in mitosis is independent of chromosomes, centrosomes, and antiparallel microtubules. *Mol. Biol. Cell.* 5:217–226.

Sawin, K.E., K. LeGuellec, M. Philippe, and T.J. Mitchison. 1992. Mitotic spindle organization by a plus-end-directed microtubule motor. *Nature.* 359: 540–543.

Shirasu-Hiza, M., Z.E. Perlman, T. Wittmann, E. Karsenti, and T.J. Mitchison. 2004. Eg5 causes elongation of meiotic spindles when flux-associated microtubule depolymerization is blocked. *Curr. Biol.* 14:1941–1945.

Vallotton, P., A. Ponti, C.M. Waterman-Storer, E.D. Salmon, and G. Danuser. 2003. Recovery, visualization, and analysis of actin and tubulin polymer flow in live cells: a fluorescent speckle microscopy study. *Biophys. J.* 85: 1289–1306.

Waterman-Storer, C.M., A. Desai, J.C. Bulinski, and E.D. Salmon. 1998. Fluorescent speckle microscopy, a method to visualize the dynamics of protein assemblies in living cells. *Curr. Biol.* 8:1227–1230.

Westerweel, J. 1997. Fundamentals of digital particle image velocimetry. *Meas. Sci. Technol.* 8:1379–1392.

Wittmann, T., and T. Hyman. 1999. Recombinant p50/dynamitin as a tool to examine the role of dynactin in intracellular processes. *Methods Cell Biol.* 61:137–143.